J Braz. Soc. Mech. Sci. Eng. (2017) 39:4367–4378
DOI 10.1007/s40430-017-0753-5

TECHNICAL PAPER

Automatic shape optimization of a conical-duct diffuser using a distributed computing algorithm

Nicolás Herrera[1] · **Sergio Galván**[1] · **Juan Camacho**[2] · **Gildardo Solorio**[1] · **Alicia Aguilar**[1]

Received: 23 July 2016 / Accepted: 4 March 2017 / Published online: 23 March 2017

Abstract In a hydraulic turbine, approximately three quarters of the energy recovery by the draft tube are obtained at the runner outlet, in its conical part. The performance of this component is a strong function of many flow variables as well as geometric aspects. Until now, different cone geometries have been created by changing lengths, diffuser angles, or shapes. However, the best cone angle for a specific inlet flow, shape, and length has not been well established. Moreover, there is a lack of information in terms of the exact position of the opening angle of a conical-duct shape diffuser to give the highest performance. To find this angle, an automatic optimization process manipulated by the Multi-Island Genetic Algorithm was created to generate different diffuser geometries to be evaluated through CFD simulations. Its computational cost has been overcome using a distributed computing evaluation established in a computational cluster. The methodology has allowed the location of the exact opening angle, improving approximately 1.2% the diffuser performance. A quantitative and qualitative analysis of the flow has been undertaken to understand how the optimum opening angle of a diffuser modifies the flow pattern to achieve the highest performance.

Keywords Hydraulic turbine · Conical-duct diffuser · Automatic numerical optimization · CFD · Multi-Island Genetic Algorithm

1 Introduction

In hydropower plants, the potential energy of the water contained in dams is harnessed by means of hydraulic turbines in which the draft tube is one of the most important devices. Its function is to reduce the pressure in the outlet of the runner through a suction head, and also reduce the losses of the overall process by converting the kinetic energy of the runner outlet flow into pressure. Draft tube features typically comprise an inlet cone, a bend, and an outlet leg; in fact, approximately three quarters of the energy recovery are obtained at the runner outlet, in the conical part.

Its performance is highly dependent on the conditions of the inlet flow and its design parameters; diffuser angle or area ratio, length, and shape of the cross section. Through these parameters, a better performance may be obtained either by increasing the amount of diffusion, decreasing any non-uniformity in the velocity profile, or making the diffusion more efficient, thereby reducing overall losses across the diffuser [25].

Technical Editor: Jader Barbosa Jr.

✉ Sergio Galván
srgalvan@umich.mx

Nicolás Herrera
nikohs85@gmail.com

Juan Camacho
jccamachoarr@gmail.com

Gildardo Solorio
gdiaz@umich.mx

Alicia Aguilar
aliac77@hotmail.com

[1] Mechanical Engineering Department, Universidad Michoacana de Sán Nicolás de Hidalgo, Apdo. Postal 588, Morelia, Michoacán CP 58000, Mexico

[2] Tecnológico Nacional de México, Instituto Tecnológico de Morelia, Av. Tecnológico 1500, Lomas de Santiaguito, Morelia, Michoacán, Mexico

Alternatively, when the space is marginal, different diffuser shapes are worthy of consideration. For example, using shorter diffusers could be particularly effective to delay the flow velocity followed by a parallel pipe to make the flow uniform. For this reason, its diffusion effectiveness should depend on the maximum opening angle of the conical section or the conical-duct relation. However, the combination of several design parameters and research dimension space would make impossible to find out the exact angle and position where the conical duct will develop its maximum performance.

To resolve this kind of problem, optimization algorithms have been coupled to CFD analysis showing good results. Recently, only the flow conditions have been controlled by manipulating eight parameters of the inlet velocity profiles to yield better draft tube cone performance [10, 13]. Marjavaara [19] presented three examples of draft tube shape optimizations based on CFD and surrogate models. Eisinger and Ruprecht [4] developed a mathematical algorithm to automatically optimize hydro turbines components and showed another three examples of geometry optimization of draft tubes using three different optimization algorithms: search directions (EXTREM method), discrete SIMPLEX type methods, and genetic algorithms. Soni et al. [26] present a study in which by proposing several geometry modifications of a draft tube and by means of CFD analysis, they found the optimized design. Marjavaara and Lundström [20] used response surface methods (RSM) to optimize the geometry of a Francis draft tube, showing that the RSM can offer satisfactory results in design processes of hydraulic components.

There are several optimization algorithms, but the genetic algorithms (GA) are proven to work well in hydro machinery [7] and their effectiveness has been validated [3, 16]. However, the choice of an optimization method, as the GA, will require a large number of Navier–Stokes computations to evaluate many different draft tube shapes before reaching a good solution satisfying field flow requirements. Although this procedure allows the possibility of finding an efficient design, it is expensive in terms of computational time due to the evaluation of the individual's fitness, which is the most time-consuming component of the optimization. Then, it is necessary to keep the cost and duration of the design process within reasonable limits. One solution could be the distribution of the genetic algorithm to several processing elements. A distributed model describes how different parts of the task can be calculated independently of the other parts. Thus, the distributed efficiency is extremely important, if objective function evaluation consumes most of the computational time, as is the case for draft tube numerical simulation.

Despite the fact that the previous works have used different methodologies and design variables, the optimal shape for a diffuser that is limited by the space between the outlet of the turbine and the bend of the draft tube is not evident. Indeed, [6, 15, 18] developed similar methods on the same diffuser to diverge the flow passage, maintaining the length after the diffuser to assure the proper development of the flow. Mirzaei and Babaei [23] developed a multi-objective optimization to maximize the pressure recovery and minimize the loss coefficient. The cone angle and the height above tailrace were selected as design variables. The results were influenced by the effect of the inlet flow swirl and there is no punctual value of the variable designs showing that the performance of the diffuser was augmented. All those practices merely permitted observation of the diffuser performance to determine provocation by diffusive or dissipative effect. Then, if the diffuser performance could be improved through the pressure recovery coefficient Cp, it would be convenient to manipulate both the flow uniformity and the total pressure losses. However, when one has to accept the non-uniformity in the diffuser inlet velocity profile, it is necessary to know if this profile could be improved by varying the pipe length after or before the modified divergence.

In consequence, the aim of this research is to increase diffuser performance by maximizing the pressure recovery factor, by improving the uniformity of the outlet velocity profile and by reducing the energy losses through the diffuser. To achieve this, a genetic algorithm should find the exact relation divergence duct necessary to correct the flow pattern along the diffuser using a distributed processing system. This system has been able to execute tasks on remote machines at the same time, other than the host on which the optimization manager session runs, executing each design in parallel, i.e., using several processors.

This exploratory technique has been implemented within the iSight software through the Multi-Island Genetic Algorithm (MIGA), which corresponds to an advanced version of traditional genetic algorithm approaches. With this automatic process, the best performance of a diffuser by coupling commercial computational programs should be achieved. The optimization algorithm must be capable of conveniently managing the diffuser parameters to generate a wide range of diffuser shapes through a CAD software which will be evaluated through a CFD software.

It is worth remarking that this optimization process has represented a challenge. First, the flow field inside a draft tube cone is highly three-dimensional, complex, and computationally very expensive to be modeled numerically. Second, the draft tube performance is very sensitive to the solid flow interaction, which requires that the cone shape must be correctly parameterized. Finally, cone shape optimization cycle must be subject to some required

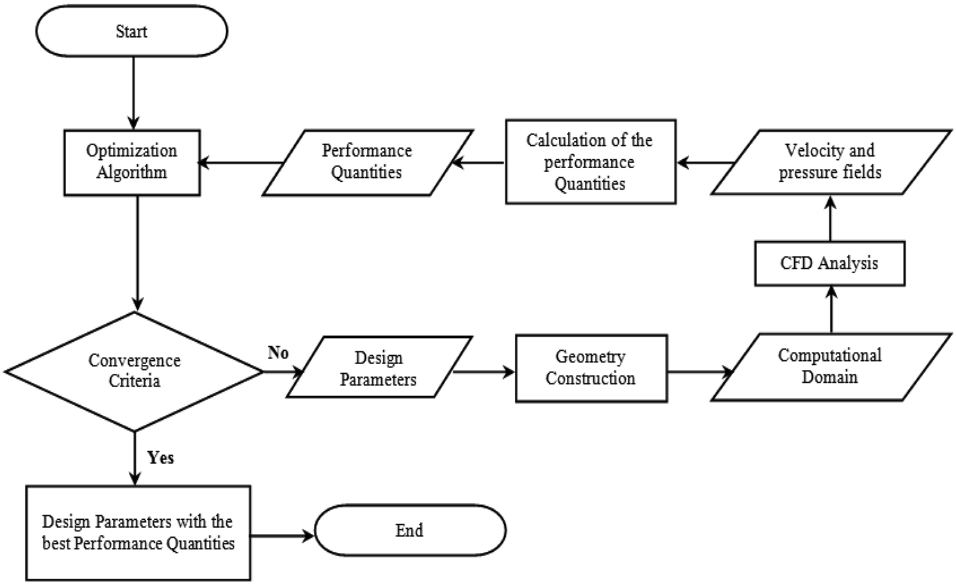

Fig. 1 Iterative solution procedure for the overall optimization process

supervision during the process and also subject to an extensive objective function evaluation.

2 Methodology

The main optimization strategy developed in this research consists of the coupling of codes of different disciplines that are executed via a shell script. This process has been configured through a graphical interface within which the user can set up, monitor, and analyze a design problem. The automatic optimization loop created for this work is shown in Fig. 1.

iSIGHT [5] generates data for the design variables, and Gambit [8] reads these values and generates a new geometry ready to be imported by Fluent [9] to execute a CFD simulation. Finally, MATLAB [27] handles the data exported by Fluent to calculate the performance of the geometry. The value obtained returns to iSight to start the process again. The optimization ends when the number of cycles programmed has been completed.

2.1 Optimization algorithm

Optimization can be defined as the process of finding the conditions that give the maximum value or minimum value of a function. The choice of a global optimization method, such as the GA, requires a large number of 3D Navier–Stokes computations to evaluate different diffuser shapes before reaching a good solution satisfying field flow requirements. Multi-Island Genetic Algorithm (MIGA), one of the distributed genetic algorithms (DGA), has been chosen to execute the search of the best diffuser shape, due to its robustness and capability to find the global optimal value and the possibility to run in a distributed manner. The main feature of MIGA that distinguishes it from the traditional GA's is the fact that each population is divided into subpopulations called islands, as it is shown in Fig. 2.

This characteristic allows the genetic operations to be performed separately on each island. Some individuals are selected from each island and migrated to different islands periodically. Multi-Island Genetic Algorithm allows preserving the best individual from the previous generation without alteration. This operation is called elitism, and it guarantees that the best genetic material is carried over the generations.

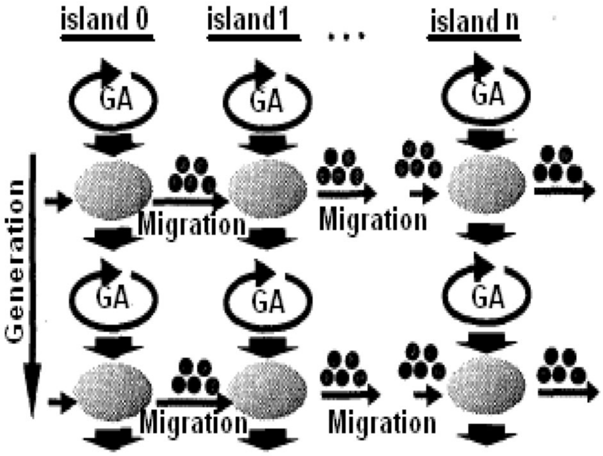

Fig. 2 Conceptual model of MIGA [10]

Table 1 Values for the basic optimization tuning parameters used in this study

Parameters	Value
Size of subpopulation	10
Number of islands	4
Number of generations	60

In Table 1, the basic optimization tuning parameters used in this study are shown. For the advanced tuning parameters, the default values remained.

The size of subpopulation is the population in each island; therefore, the total cycles are the number of individuals in each island multiplied by the number of islands, and then multiplied by the number of generations. This gives 2400 individuals that have to be analyzed to complete the process. This value represents the number of times that the cycle shown in Fig. 1 should be repeated. If the analysis for each design point (individual) is made by a CFD study, a large amount of computational time is required.

To deal with this problem, the data exchange between the CAD-CFD process (design) and the iSIGHT host was executed through a calculating network (Fig. 3). This network has the master nodes that permit access to ten calculating nodes. Each node has eight processors with 4.0 GHz and 16 GB of RAM memory, where each individual was evaluated and parallelized to reduce the computational time of each CFD calculation and of the overall process.

The average CPU time for each iteration, including the CFD analysis, was nearly 3 min. This means that in a single computer, 2400 iterations would have taken approximately 5 days. With the calculation cluster, this time was reduced dramatically to several hours.

2.2 Diffuser parameterization

In a hydraulic turbine, the principal part of energy recovery is obtained at the runner outlet in the conical part of the draft tube. There, the cone angle or area ratio increases the flow section, which determines the energy conversion from kinetic to pressure. The cone angle has been established to avoid the wall flow separation reducing the flow velocity. To achieve this condition, the location of the optimal cone opening angle must be determined.

To locate this point, the diffuser geometry has been parameterized, as shown in Fig. 4. Unlike [21] who utilized Bezier curves to define the diffuser shape, in this work, only a control point $P(y_i, z_i)$ was defined to displace the design region. This displacement with one degree of freedom will generate the opening angle θ and with two degrees of freedom, the relation conical duct. Using these two conditions, the flow behavior developed along the diffuser is expected to improve, thus enhancing its performance.

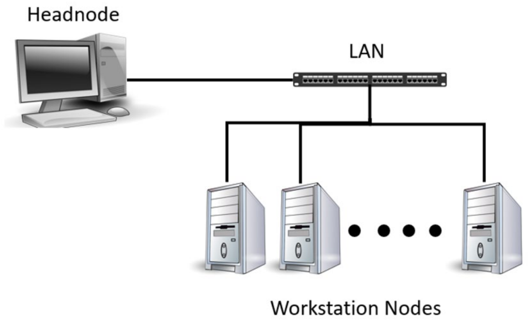

Fig. 3 Distributed and parallelized architecture of the computational cluster

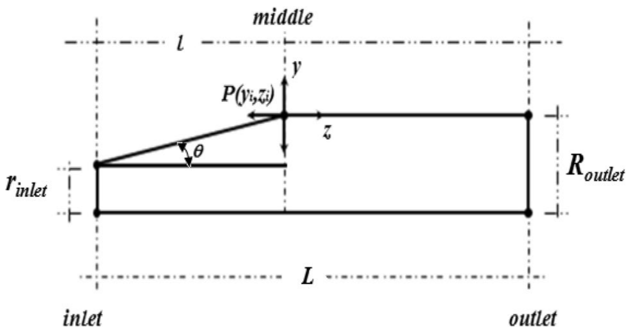

Fig. 4 Geometrical parameterization of the diffuser

From Fig. 4, we can get the area ratio in Eq. 1 which gives us the opening angle of the divergence:

$$\mathrm{AR} = \frac{A_{\text{outlet}}}{A_{\text{inlet}}}, \tag{1}$$

and Eq. 2, the length ratio, which will give us the relation conical duct:

$$\mathrm{LR} = \frac{L}{l}. \tag{2}$$

The diffuser geometry and computational domain has been developed using a Gambit [8] journal file by setting five points on the plane $y - z$. For each CFD evaluation, a 2D axisymmetric face must be created, which is then revolved to create the 3D geometry. In this way, if the point $P(y_i, z_i)$ in Fig. 4 is manipulated, it is possible to build different draft tube cone geometries with different AR and LR ratios. The same topology and mesh parameters were used to build each diffuser geometry to avoid the variation of the grid quality [20].

2.3 The objective function

To describe the diffuser performance, a number of parameters such as efficiency, loss coefficient, and pressure recovery have been defined [22]. For this task, the objective function to be maximized is the mean pressure recovery, since it applies where uniform axial flow pertains at the cone inlet. Then, the structure of the inlet velocity profiles is modified, Galván et al. [12] demonstrated through a flow sensitivity study that the loss coefficient is the most appropriate objective function for an optimization process.

Thus, the objective function to be maximized is presented in Eq. 3. This factor indicates the amount of kinetic energy that is converted into static pressure, where higher values represent a higher efficiency.

$$\mathrm{Cp_m} = \frac{\frac{1}{A_{\mathrm{out}}}\int_{\mathrm{out}} P\mathrm{d}A - \frac{1}{A_{\mathrm{in}}}\int_{\mathrm{in}} P\mathrm{d}A}{\frac{1}{2}\rho\left(\frac{Q}{A_{\mathrm{in}}}\right)} \tag{3}$$

where A is the area; P is the static pressure; Q is the flow rate; ρ is the density; and the subscripts in and out correspond to the inlet and outlet. The expression in the numerator represents the difference between the inlet and outlet static pressure, and the term in the denominator is the inlet dynamic pressure. Thus, the $\mathrm{Cp_m}$ should be monitored in response to the opening angle changes.

2.4 Numerical model

The diffuser shape and its computational domain are shown in Fig. 5. They are based on an industrial hydraulic turbine used for experiments involving swirling flow through the conical part [10, 11]. According to Fig. 4, the original conical-duct diffuser has an $AR = 4.0$ with a half angle of $\theta = 12\,^{\circ}$ and $LR = 2.27$.

In this work, the Reynolds Average Navier–Stokes and the $\kappa - \varepsilon$ turbulence model equations were used to describe an incompressible, viscous, turbulent, and steady flow, [12]. The standard model has been shown to be economical, robust, and reasonably precise, but it gives poor results for complex fluxes with severe pressure gradients, strong streamline curvature, swirl, and rotation, like the one in a draft tube. However, during an optimization process where fine details of flow characteristics are not required the standard turbulence model, $\kappa - \varepsilon$ was confirmed as reliable and robust and able to study the effects of mildly swirling flow through the turbine draft tube [14].

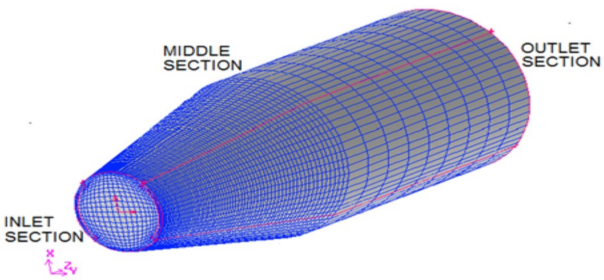

Fig. 5 Computational domain of the conical-duct diffuser [10]

These equations were solved using the commercial program FLUENT which is based on the Finite Volume Method and the pressure velocity coupling. The geometry and the computational grid were edited using GAMBIT for boundary specifications. A grid with 42,840 cells designed for near-wall treatment was used. At the inlet section, the velocity field was imposed using three velocity components and constant turbulent quantities were imposed. The radial distribution of the circumferential component was established using a free vortex approach and the axial component had a uniform radial distribution, which resulted in a flow rate of $Q = 0.7727\ \mathrm{m^3/s}$. In addition, constant turbulent quantities, an average turbulent intensity $I = u'/u_{\mathrm{ave}} = 4.98\%$, and an average relative viscosity $\mu'/\mu_{\mathrm{t}} = 99.40$ were established as inlet turbulence boundary conditions. At the outlet, a constant pressure boundary condition is used. The standard logarithmic rough wall function has been imposed at the walls with $y^{+} = 67.4416$. The surface roughness is set to $10\ \mu\mathrm{m}$ at the cone wall. The fluid density was set to $998.2\ \mathrm{kg/m^3}$ and the dynamic viscosity $1.004^{-6}\ \mathrm{m^2/s}$.

Using the same CFD setup for the original diffuser geometry, [10] applied a numerical optimization process to minimize the flow energy losses. In that study, the analytical velocity distribution at the inflow section of a draft tube presented by [24] was used to accurately capture the velocity profile of the original diffuser with three different analytical vortex systems. The radial distribution of the inlet vortex system was optimized, which gave rise to different flow configurations along this device. The study includes a discussion on the development of the flow structure with the aim of understanding its impact on the diffuser performance. In the same way, it is expected that the analysis of the flow behavior in the geometries obtained from the shape optimization process will help us to understand the dominant effect that the geometric parameters have on the flow development along the diffuser.

2.4.1 *Grid convergence error*

According to [1], it is possible to estimate a global performance quantity, by means of the equation:

$$\phi_{\mathrm{ext}} = \frac{\alpha_2^{p}\phi_h - \phi_{\alpha_2 h}}{\alpha_2^{p} - 1} \tag{4}$$

where ϕ is the performance quantity, (Cp_m in our case), h is the grid cell size, p is the order of the method, and α is the grid refinement factor, which is defined by the following:

$$\alpha = \left(\frac{N_1}{N_2}\right)^{\frac{1}{3}}. \tag{5}$$

In this formula, N_1 is the grid size number for the finest grid, and N_2 for the coarser grid. The order of the method p should be between 1 for a first-order discretization scheme and 2 for a second one. Thus, the global variable performance obtained by the Richardson's extrapolation for both schemes is shown in Table 2.

The grid error was estimated using

$$e_r = \frac{\phi_{ext} - \phi_h}{\phi_{ext}}. \tag{6}$$

The errors e_1 and e_2 for different grid sizes are shown in Table 3 if p is assumed to be 1 and 2.

The final $e_2 = 9.05\%$ for the grid N_5 can be considered as an acceptable error, because [2] estimated an until 30% for this kind of error.

A plot of the global performance quantity for the five grid sizes is shown in Fig. 6. The curves are obtained by solving for η in the following:

$$\phi(\alpha) = \phi_{ext} + \eta\alpha^p \tag{7}$$

where:

$$\eta = \frac{\phi_{ext} - \phi_h}{h^p}. \tag{8}$$

For Cp_m, the five grids are inside this range, as shown in Fig. 6. Thus, an attempt to reduce the CFD time is to substitute the fine diffuser grid size, N_5 by a coarse one N_1 with a much lower computational cost.

Table 2 Extrapolated value ϕ_{ext} of the engineering quantity using both discretization schemes order; first $p = 1$ and second $p = 2$

$\phi_{ext}(Cp_m)$	
($p = 1$)	($p = 2$)
0.893161	0.892908

3 Results and discussion

A shell script controls the automatic optimization process to generate the diffuser geometries. Each geometry is evaluated through a CFD simulation obtaining the pressure and velocity fields. These results are processed to get the objective function (Cp_m) value. The objective function behavior with respect to each evaluation is presented in Fig. 7. The objective function is plotted for each individual of each generation versus the index of iteration. Figure 7a indicates that the convergence has been reached with $Cp_m = 0.9050$ after 2400 runs. This study was performed just modifying $P(y_i)$ along the y coordinate. This variation allowed finding the best opening angle by modifying the area ratio (AR) without any change of the length ratio LR. Figure 7b shows the history of the objective function when the control point is manipulated on the $y-z$ plane, i.e., changing the length ratio LR. Only 360 evaluations were necessary to achieve the $Cp_m = 0.9070$.

Table 4 presents the final diffuser parameters reached due to the manipulation of the control point through the MIGA. Even though the original design is an optimal diffuser, the final value of the objective function for each optimized diffuser shape has been higher than that obtained using the original geometry. Thus, the optimization process was able to accomplish an additional increment of around 1.14 and 1.37% in the effectiveness of the diffuser ($Cp_m x$) in recovering the kinetic energy entering to it.

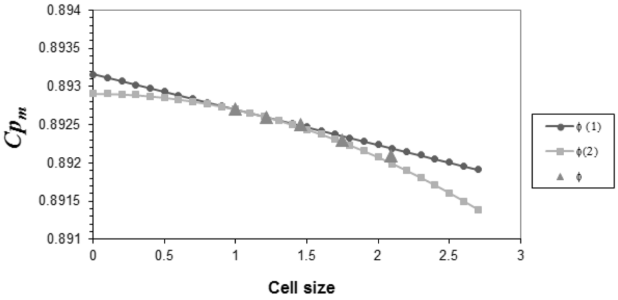

Fig. 6 Plot of the mean pressure recovery coefficient quantities using the Richardson extrapolation method, with a first-order scheme $\phi(1)$ and a second order scheme $\phi(2)$

Table 3 Grid error estimated in percent for the five grid size and the scheme order; first e_1 and second e_2.

	Grid	1	2	3	4	5
Cp_m	N	390,279	216,678	125,388	72,732	42,840
	α	1.0000	1.2167	1.4600	1.7506	2.0884
	ϕ	0.8927	0.8926	0.8925	0.8923	0.8921
	e_1	0.0516	0.0628	0.0740	0.0964	0.1188
	e_2	0.0233	0.0345	0.0457	0.0681	0.0905

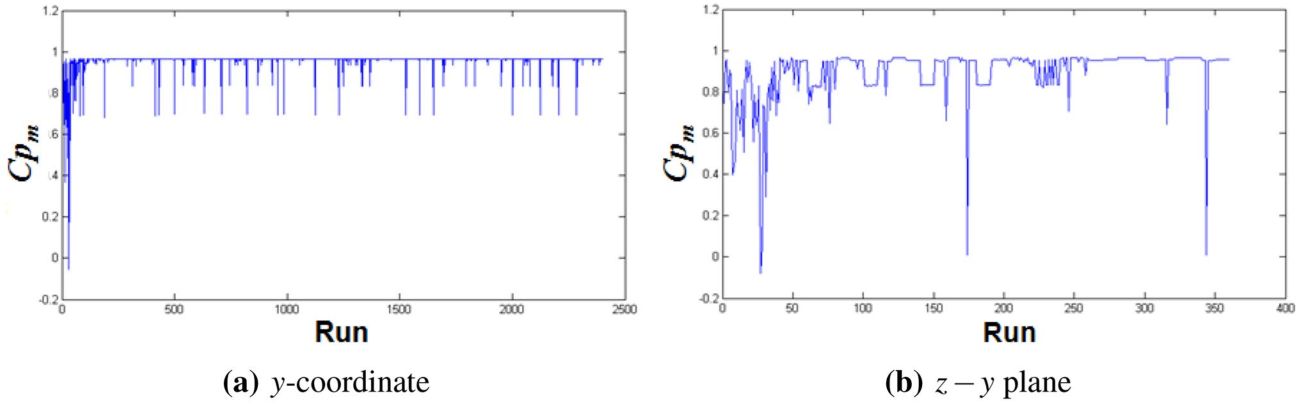

(a) *y*-coordinate **(b)** $z-y$ plane

Fig. 7 Optimization history of the objective function during the process

Table 4 Comparison of the $\mathrm{Cp_m}$ values and design variables reached for each diffuser

Design	θ	AR	LR	$\mathrm{Cp_m}$	Gain %
Original	12.0	4.0	2.27	0.8948	–
y-coordinate	13.17	4.41	2.27	0.9050	1.14
$y-z$ plane	13.10	4.53	2.20	0.9070	1.37
Inlet velocity	12.00	4.0	2.27	0.9125	1.98

The new diffuser parameters obtained by this optimization process are shown from the second to fourth column of the Table 4, which resulted from manipulating only one control point. The manipulation of only a design parameter notably reduced the computational cost of the optimization process. These results present enough evidence to prove that the angle of the cone has a high impact on the draft tube performance and knowing its exact value and position could be of great interest for designers searching for a higher performance of the draft tube.

Figure 8 compares the flow behavior of the axial velocity provoked by the optimized geometries, which, in turn, had been provoked by an optimized inlet velocity profile. The optimized diffuser geometries show an increment of the near-wall region where the axial velocity is very low. This effect could be harmful, because the positive axial pressure gradient created would provoke flow separation or near separation. Instead, the principal gain of this new shape configuration is the reduction of the amplitude of the very low flow along the core region. The new flow structure obtained enables visualization of the flow, as it tends to increase the axial velocity along the core region. This flow structure could be extrapolated to a real draft tube, and we can assume that this reduction would prevent stagnation, or even reversal of the velocity beneath the runner. In the optimized inlet velocity, the radial distribution of the axial component at the inlet reaches a peak in the core, and the circumferential component is a profile with one or two Batchelor vortices [10].

Figure 9 revels the flow deceleration along the three survey sections. For the optimized geometries, in the middle section, Fig. 9b, the tangential velocity has a high value in a larger section of the radius. This phenomenon helps to keep the ow attached to the wall. In addition, the increment of the tangential velocity intensity in the core section provoked by the optimized velocity prole is evident. At the outlet section, Fig. 9c, the velocity profiles generated by the optimized geometries are very similar, except for the optimized velocity profile with higher values along the radius.

In Fig. 10, the distribution of the total pressure is indicated on each cross section of the diffuser. For a change of AR, and AR and LR, there is a pressure zone at the center that is conserved downstream. Both diffuser configurations achieve a favorable total pressure gradient near the wall that maintains a more uniform pressure at the outlet section than that reached by the original diffuser design, Fig. 10c. This effect would imply a better diffuser performance. Consequently, in the outlet section, the pressure near the center is not much different from that at the wall. Comparing the radial pressure distribution in the inlet section with those in the downstream sections, it is clear that the first presents a significant radial gradient where the pressure is higher near the wall. Thus, the fluid in the core does not have enough energy to flow downstream, except for that generated by the optimized inlet velocity profile (Fig. 8), and it is pulled forward by the fluid surrounding it. The effective cross-sectional area is reduced and a higher total pressure loss should result.

Figure 11 shows the evolution of the turbulent kinetic energy in the three survey sections of the diffuser. It can be seen that all geometries obtain the energy dissipation of the flow in the centre of the diffuser. However, the new

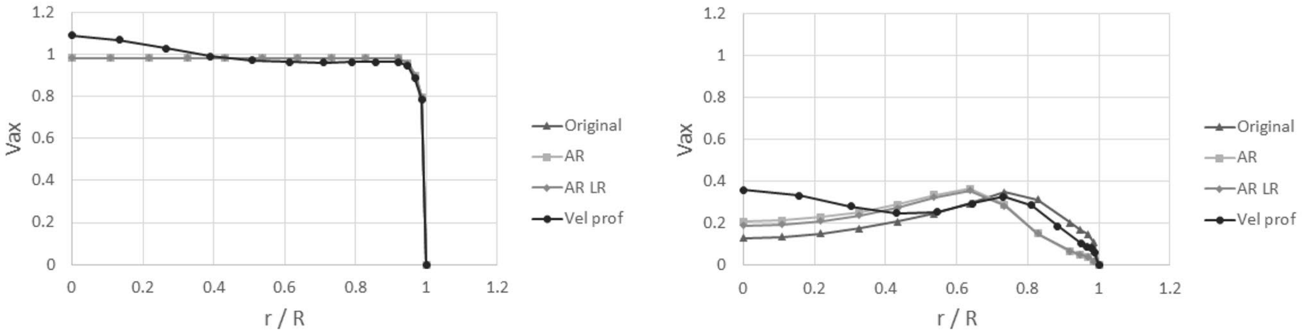

(a) Inlet **(b)** Middle

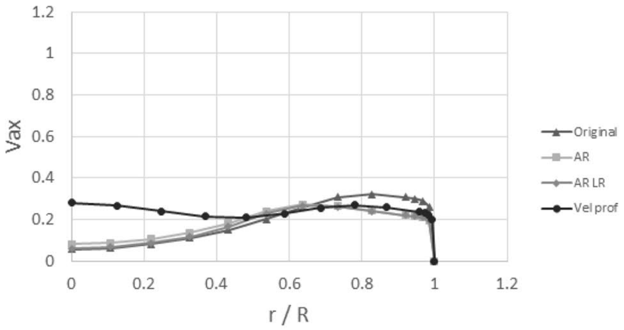

(c) Outlet

Fig. 8 Plots of the normalized axial velocity component on three planes

diffuser geometries provokes important differences in the near-wall region in the middle Fig. 11b and the outlet Fig. 11c sections. The modifications of both geometrical parameters seem to incite a more significant production of turbulent kinetic energy near the wall than that obtained for the original diffuser and by an optimized inlet velocity profile. Thus, the turbulent kinetic energy in both cases of the optimized geometries still exists at the end of the diffuser.

To better understand the mechanisms of the diffusion and the dissipation and its effects on the diffuser performance, Sharan [25] researchers measured the static pressure recovery in conical diffusers using the following equation:

$$\mathrm{Cp} = \alpha_{\mathrm{in}}\left[1 - \frac{\frac{\alpha_{\mathrm{out}}}{\alpha_{\mathrm{in}}}}{\mathrm{AR}^2}\right] - \zeta \tag{9}$$

where:

$$\alpha_{\mathrm{in/out}} = \frac{1}{\mathrm{AV}^3}\int_A v_{\mathrm{a}}^3 \mathrm{d}A \tag{10}$$

where α is the kinetic-energy flux parameter and represents the non-uniformity of the velocity profile, V is the average velocity, A the survey area, v_{a} represents the axial component, and ζ are the total pressure lost as the flow travels downstream, and it is defined as:

$$\zeta = \frac{\frac{1}{A_{\mathrm{in}}}\int_{\mathrm{in}} P_{\mathrm{t}}\mathrm{d}A - \frac{1}{A_{\mathrm{out}}}\int_{\mathrm{out}} P_{\mathrm{t}}\mathrm{d}A}{\frac{1}{2}\rho\left(\frac{Q}{A_{\mathrm{in}}}\right)^2} \tag{11}$$

where P_{t} is the total pressure, and A_{in} and A_{out} the diffuser area at the inlet and outlet, respectively. The total pressure is given by:

$$P_{\mathrm{t}} = P + 0.5(u^2 + v^2 + w^2) \tag{12}$$

with u, v, and w as the Cartesian components of the velocity.

The Eq. 9 shows that the static pressure recovery depends upon two factors: the diffusion and the dissipation. The diffusion is defined by the first term, and it is due to the inlet and exit velocity profiles shapes ($\alpha_{\mathrm{out}}/\alpha_{\mathrm{in}}$). The second term represents the overall losses occurring within the diffuser as a result of the viscous effects. The above equation shows that diffuser performance may be improved by having uniform flow or by reducing overall losses.

Table 5 compares the dissipative and the diffusive terms obtained from the optimized shapes against the

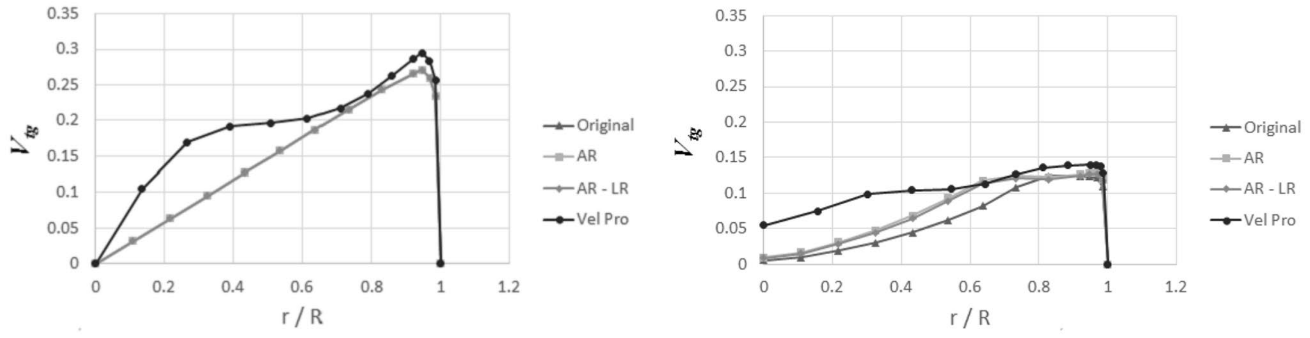

(a) Inlet **(b)** Middle

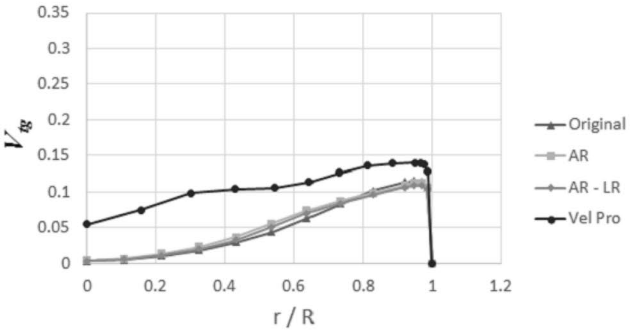

(c) Outlet

Fig. 9 Plots of the normalized tangential velocity component on three planes

original and those obtained by the optimization of the inlet velocity profile using Eq. 9. The effect of the non-uniformity in the velocity profiles converts ($\alpha_{\text{out}}/\alpha_{\text{in}}$) greater than unity, as is presented by the original diffuser. The optimized diffuser shapes improve this value, but the one reached by the optimized inlet velocity profile is the best. In addition, it is shown that the levels of diffusion were upgraded for the optimized shapes through the uniformity of the velocity profile, but its dissipative part was seriously deteriorated. Then, the geometrical effect delivered by the AR parameter shows to be highly important to compensate the velocity profile distortion and the total pressure loss across the diffuser. Thus, the gains obtained with the design-shape optimization of the diffusers, calculated with Eq. 9, are about 2%.

To understand the draft tube performance, the behavior of some engineering quantities was evaluated. The amount of kinetic energy of the tangential velocity component was quantified with the coefficient α_{tg} and also the swirl intensity of the flow along the diffuser was obtained using the swirl number S.

Physically, α_{tg} represents the ratio of the actual kinetic-energy flux, at a given cross section of an internal flow stream, to the minimum kinetic-energy flux which could exist at a particular flow rate. It is given by:

$$\alpha_{\text{tg}} = \frac{1}{AV^3}\int_A {v_{\text{t}}}^2 v_{\text{a}} \mathrm{d}A \tag{13}$$

where v_{a}, v_{r} and v_{t} are the polar components of the velocity.

The swirl number S is defined as the axial flux of swirl momentum divided by the axial flux of axial momentum:

$$S = \frac{\int_0^R (\rho v_{\text{a}})(r\, v_{\text{t}})\, r\, \mathrm{d}r}{R\int_0^R (\rho\ v_{\text{a}})(r\ v_{\text{a}})\, \mathrm{d}r}. \tag{14}$$

Figure 12a shows the development of α_{tg} through the cone. The geometries and the velocity profile profiles caused an augmentation of this energy before the middle section and a little reduction after it. The possibility of modifying both geometrical parameters LR and AR provoked an important reduction of this energy at the end of the diffuser. The swirl intensity along the diffuser is presented in Fig. 12b. The optimized geometries and inlet velocity profile increased the swirl level downstream, inversely the original profile reduced its swirl intensity at the end of the diffuser. The increase of swirl in this part of the device would avoid fluid separation from the wall which induces a lower energy loss.

These results have demonstrated that the optimization shape design methodology seems to be reliable for

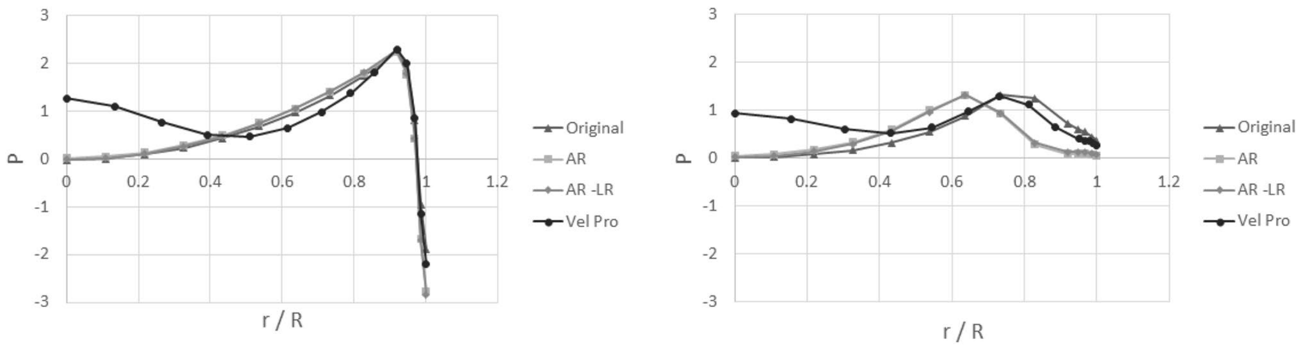

(a) Inlet **(b)** Middle

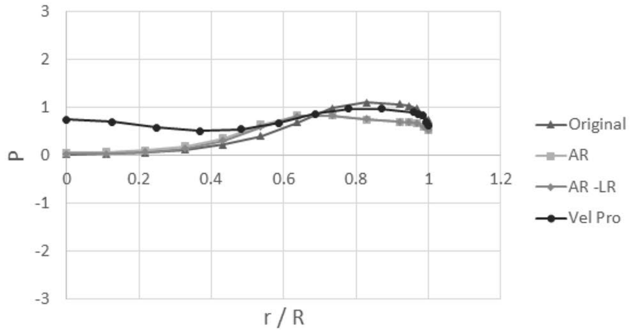

(c) Outlet

Fig. 10 Plots of the normalized total pressure on three planes

maximizing the energy recovery of the of a conical-duct diffuser. The first optimization found the exact opening angle moving the control point along the *y* coordinate. The second optimization found the best relation $AR - LR$ to maximize the objective function.

Equations 3 and 9 have estimated a range of parameters to achieve the best cone performance that was improved 1.2% in relation to the original design. The latter finding is particularly important, because [17] estimated that only 0.006% of improvement in the draft tube dramatically changes the overall performance of a hydraulic turbine until 0.5%.

The qualitative results have also been useful for evaluating the efficient diffusion of the optimized diffuser shapes. Using the same axial velocity profile at the inlet, the optimized diffuser produced a reduction in the velocity level of the fluid stream and an increase in its static pressure.

The effect of increasing the area ratio provoked a high degree of dissipation in the draft tube; however, the diffusion reached was enough to improve the Cp. In the velocity profile optimization, the dissipation was minimized only improving the uniformity of the velocity profile obtaining the better gains. Then, it has been demonstrated that the AR parameter has an important impact on the performance of the diffuser. However, when the diffuser is part of the draft tube and its length and area ratio are impossible to change, the only option is to find the shape and LR ratio which improve the dissipation and reduce the losses through this component.

Finally, since much of the basic research on diffuser performance apply directly to draft tubes, the knowing of the exact value of the angle and its position could be of great interest for the designers searching for a higher performance of this turbine device.

4 Conclusions

This study presented an automated design-shape optimization methodology that reached the maximum performance of a conical-duct diffuser through the exact localization of the AR and LR parameters. On the basis of the numerical work reported herein, the following conclusions may be drawn concerning the flow development in conical-duct diffusers. The gains obtained with a little change of its design parameters were about 1.14 and 1.37%. However, they were lower than those obtained when only the inlet velocity profile was optimized.

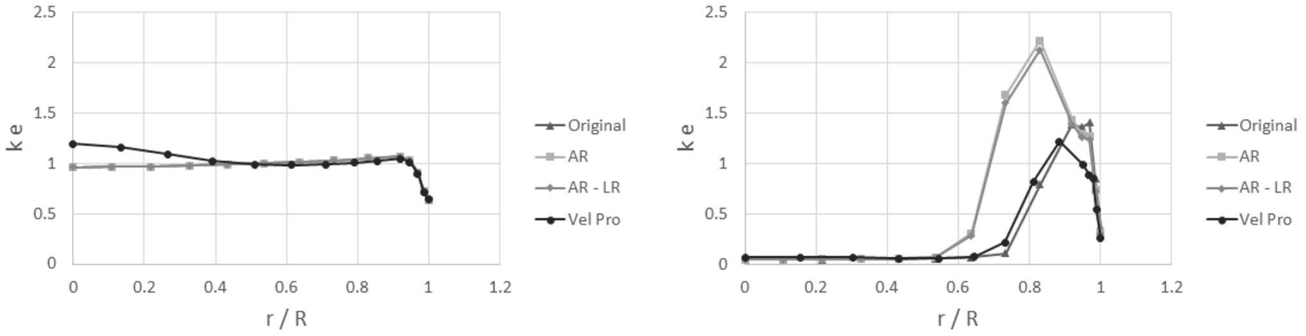

(a) Inlet **(b)** Middle

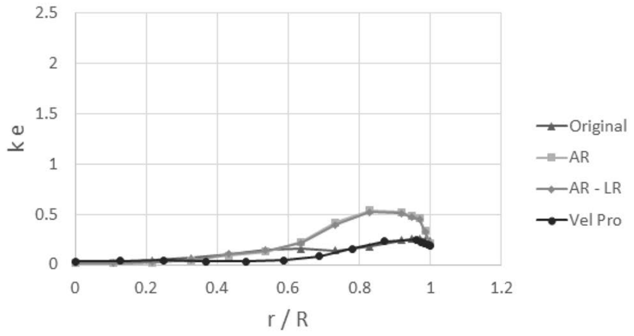

(c) Outlet

Fig. 11 Plots of the normalized kinetic energy on three planes

Table 5 Detailed performance values reached for each diffuser

Design	$\alpha_{\text{out}}/\alpha_{\text{in}}$	AR	Diffusive	Dissipative	Cp	Gain %
Original	1.29	4	0.9146	0.0323	0.8823	–
y-coordinate	1.15	4.41	0.9353	0.0360	0.8993	1.93
$y{-}z$ plane	1.19	4.53	0.9365	0.0364	0.9001	2.02
Inlet velocity	0.92	4	0.9368	0.0316	0.9052	2.60

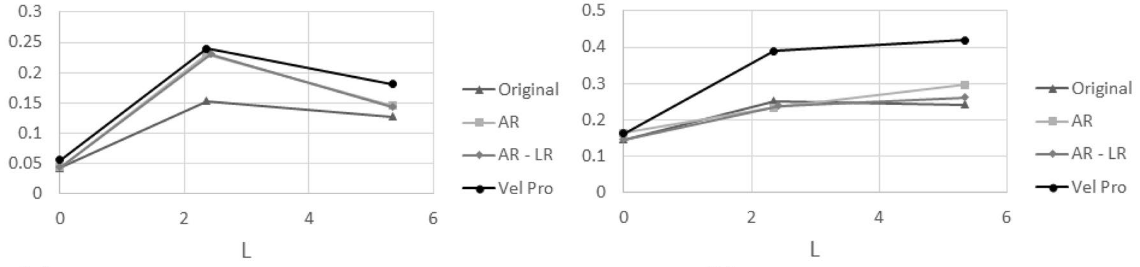

(a) Tangential kinetic energy correction factor. **(b)** Swirl intensity.

Fig. 12 Engineering quantities behavior along the length diffuser L (m)

With this study, it has also been possible to identify the flow structure by means of which the diffuser performance was affected both quantitatively and qualitatively. The diffusion effect has been improved particularity by the AR parameter, although the dissipation effects were increased importantly. Further research might try to improve the diffusion effect maintaining the AR constant but searching for the exact position of the LR parameter to increase flow uniformity.

Although the results obtained by this diffuser shape optimization methodology are promising, some caution must be taken into account. First, the scope of this study is limited by the selection of the advanced tuning parameters of the MIGA that could improve the optimization process. Second, the resulting inlet velocity profiles provided by a real blade runner geometry could be so different from that used in this study that this methodology could be limited only to the optimization of the diffuser with certain inlet flow characteristic. And, third, although it is known that the standard $k-e$ turbulence mode fails to capture the features of the flow along the diffuser, during an optimization process, where fine details of flow characteristics are not required, this model has been confirmed as reliable and robust and able to study the effects of mildly swirling flow through the turbine draft tube.

Finally, the authors think that the methodology and the findings developed in this study have important implications for future optimization practices. The first implication is the methodology, which is based on the coupling of commercial software that could be applied to analyze other turbo-machinery components managed by the numerical tools presented here. The second implication is that when the space is marginal, the location of the exact opening angle of the diffuser could dramatically change the overall performance of a hydraulic turbine. Then, it could be particularly effective to use shorter diffusers with large angles to delay or prevent flow separation.

Acknowledgements The authors gratefully acknowledge the CONACYT for the scholarship support to the main author and the *Coordinación de la Investigación Científica* of the *Universidad Michoacana de San Nicolás de Hidalgo* for the financial support to built the computational cluster.

References

1. Bergström J (2000) Approximations of numerical errors and boundary conditions in a draft tube. In: Turbine-99 (workshop): 20/06/1999-23/06/1999. Luleå tekniska universitet, Luleå
2. Bergström J (2000) Modeling and numerical simulation of hydro power flows. PhD thesis, University of Technology
3. Derakhshan Sh, Mostafavi A (2011) Optimization of GAMM Francis turbine runner. World Acad Sci Eng Technol 59:717–723
4. Eisinger R, Ruprecht A (2002) Automatic shape optimization of hydro turbine components based on CFD. TASK Q 6(1):101–111
5. Engineous Software Inc. (1994) Products. Isight
6. Fares R, Chen X, Agarwal R (2011) Shape optimization of an axisymmetric diffuser and a 3D hydro-turbine draft tube using a genetic algorithm. AIAA Paper, p 1243
7. Ferrando López L (2006) Surface parameterization and optimum design methodology for hydraulic turbines
8. Fluent Inc. (2007) Gambit
9. Fluent Inc. (2016) Fluent
10. Galván S, Reggio M, Guibault F (2015) Numerical optimization of the inlet velocity profile ingested by the conical draft tube of a hydraulic turbine. J Fluids Eng 137(7):071102
11. Galván S, Rubio C, Pacheco J, Gutierrez C (2011) 3d turbulent flow validation using an analytical inlet velocity profile on an industrial conical diffuser. In: VII international scientific conference MAS XXI
12. Galván S, Rubio C, Pacheco J, Mendoza C, Toledo Miguel (2013) Optimization methodology assessment for the inlet velocity profile of a hydraulic turbine draft tube: part I—computer optimization techniques. J Glob Optim 55(1):53–72
13. Galván S, Rubio C, Pacheco J, Solorio G, Carbajal Georgina (2013) Optimization methodology assessment for the inlet velocity profile of a hydraulic turbine draft tube: part II—performance evaluation of draft tube model. J Glob Optim 54(4):729–749
14. Galvan SR (2007) Optimization of the inlet velocity profile of the turbine 99 draft tube, vol 68
15. Ghosh S, Pratihar DK, Maiti B, Das PK (2010) An evolutionary optimization of diffuser shapes based on CFD simulations. Int J Numer Methods Fluids 63(10):1147–1166
16. Grafenberger P, Parkinson E, Georgopoulou C, Kyriacou S, Giannakoglou K (2008) Constrained multi-objective design optimization of hydraulic components using a hierarchical metamodel assisted evolutionary algorithm. part 2: applications. In: 24th IAHR symposium on hydraulic machinery and systems, Foz do Iguassu, Brazil, Citeseer
17. Hellström JGI, Marjavaara BD, Lundström TS (2007) Parallel CFD simulations of an original and redesigned hydraulic turbine draft tube. Adv Eng Softw 38(5):338–344
18. Jens Madsen I, Shyy W, Haftka RT (2000) Response surface techniques for diffuser shape optimization. AIAA J 38(9):1512–1518
19. Marjavaara D (2006) CFD driven optimization of hydraulic turbine draft tubes using surrogate models. PhD thesis, Division of Fluid Mechanics, Luleå University of Technology
20. Marjavaara D, Lundström S (2007) Response surface-based shape optimization of a Francis draft tube. Int J Numer Methods Heat Fluid Flow 17(1):34–45
21. Moravec P, Hliník J, Rudolf P (2016) Optimization of hydraulic turbine diffuser. In: EPJ web of conferences, vol 114. EDP Sciences, Les Ulis, pp 02079
22. Moses HI (1986) Diffuser performance for draft tube applications. In: Waterpower85. ASCE, Reston, pp 1218–1227
23. Mirzaei A, Babaei A (2014) Shape optimization of draft tubes for Agnew microhydro turbines. Energy Convers Manag 79:681–689
24. Romeo SR, Ciocan GD, Anton I, Avellan F (2006) Analysis of the swirling flow downstream a francis turbine runner. J Fluids Eng 128(1):177–189
25. Sharan KV (1976) An exponential investigation of the behaviour of conical diffusers in turbulent flow. Zeitschrift für angewandte Mathematik und Physik ZAMP 27(4):447–462
26. Soni V, Roghelia A, Desai J, Chauhan V (2010) Design development of optimum draft tube for high head Francis turbine using CFD. In: 4th international conference on fluid mechanics and fluid power, IIT Madras, Chennai, India, pp 16–18
27. The Math Works, Inc. (2005) Matlab